Anomalously Low Negative Cloud-to-Ground Lightning Flash Rates in Intense Convective Storms Observed during STERAO-A

TIMOTHY J. LANG AND STEVEN A. RUTLEDGE

Department of Atmospheric Science, Colorado State University, Fort Collins, Colorado

JAMES E. DYE AND MARTIN VENTICINQUE

Mesoscale Microscale Meteorology Division, National Center for Atmospheric Research, Boulder, Colorado

PIERRE LAROCHE AND ERIC DEFER

Office National d'Etudes et de Recherches Aérospatiales, Chatillon, France

(Manuscript received 9 October 1998, in final form 12 January 1999)

ABSTRACT

Concurrent measurements from the CSU-CHILL multiparameter Doppler radar, the Office National d'Etudes et de Recherches Aérospatiales VHF lightning interferometer, and the National Lightning Detection Network, obtained during phase A of the Stratosphere–Troposphere Experiments: Radiation, Aerosols, Ozone (STERAO-A) field project, provided a unique dataset with which to study the relationships between convective storm microphysics and associated lightning. Two storms have been examined in detail in this study: 10 and 12 July 1996. Both storms were long lived, existing in some form for over 4 h apiece, and produced very low cloud-to-ground (CG) lightning flash rates, in particular negative CG flash rates (generally <1 min^{-1} and often no CG flashes for periods ranging from 10 to almost 30 min), during all or a portion of their lifetimes while simultaneously producing relatively high intracloud (IC) flash rates (>30 min^{-1} at peak). For both storms, radar reflectivity intensity and the production of hail were anticorrelated with the production of significant negative cloud-to-ground lightning. These observations are shown to be consistent with an elevated charge hypothesis and suggest a possible way of correlating updraft speed, hail, and storm severity to CG and IC flash rates.

1. Introduction

The typical isolated airmass thunderstorm, or the typical cell within a nonsevere multicellular system, lasts less than 2 h and becomes electrically active after vigorous convective growth (Workman and Reynolds 1949; Mazur et al. 1986; Goodman et al. 1988; Williams et al. 1989b; Weber et al. 1993; Carey and Rutledge 1996). Its first flash usually is an intracloud (IC) flash, and cloud-to-ground (CG) flashes tend to not occur until later after several ICs have occurred (Workman and Reynolds 1949; Livingston and Krider 1978; Goodman et al. 1988; Williams et al. 1989b; Maier and Krider 1986). Cloud-to-ground flashes tend to peak as the main core of the cell descends to lower levels, after IC flashes have peaked (Larson and Stansbury 1974; MacGorman et al. 1989; Goodman et al. 1988, 1989; Williams et al. 1989b; Carey and Rutledge 1996).

Total flash rates in these nonsevere cells are variable but typically are less than 10 min^{-1} (Livingston and Krider 1978; Piepgrass et al. 1982; Williams et al. 1989a,b; Carey and Rutledge 1996). Cloud-to-ground flash rates generally average up to 2 min^{-1}, with peaks sometimes at higher values, over 10 min^{-1} (Maier and Krider 1982; Peckham et al. 1984; Williams et al. 1989b; Carey and Rutledge 1996).

During the midlatitude warm season the predominant ($>90\%$) polarity of cloud-to-ground lightning is negative (e.g., Orville 1994; Orville and Silver 1997), and nonsevere cells produce CGs of predominantly negative polarity, except sometimes during their dissipating stage (Fuquay 1982). However, many studies have shown that severe thunderstorms that produce large hail (diameter ≥ 2 cm), and sometimes tornadoes, often are characterized by production of predominantly positive CG lightning for extended periods (≥ 30 min) during their mature phase (Reap and MacGorman 1989; Branick and Doswell 1992; Curran and Rust 1992; Seimon 1993; MacGorman and Burgess 1994; Stolzenburg 1994; Ca-

Corresponding author address: Timothy J. Lang, Department of Atmospheric Science, Colorado State University, Fort Collins, CO 80523.
E-mail: tlang@olympic.atmos.colostate.edu

rey and Rutledge 1998). These studies show that the positive CGs are produced in rates and areal densities comparable to negative CGs in more ordinary, nonsevere convection. In a review of previous studies, Williams (1999, manuscript submitted to *Severe Local Storms, Meteor. Monogr.*) noted that many severe storms are characterized by enhanced total flash rates (usually >30 min^{-1}) and high percentages of positive CG lightning flashes. Severe storms also can produce significant negative CG lightning, as well as high total CG flash rates, up to 20 min^{-1} or more at peak (e.g., Knapp 1994).

However, there appears to be a class of thunderstorms that do not fit into the aforementioned conceptual models. These storms are intense or severe, but are characterized by low (<1 min^{-1}) negative CG lightning flash rates during all or a portion of their life cycles, without any noticeable enhancement of positive CGs (MacGorman et al. 1989; Billingsley and Biggerstaff 1994; Maddox et al. 1997). Even the positive CG storm studied by Carey and Rutledge (1998) underwent an electrically active intensifying phase that featured almost no CG lightning of any polarity for about an hour.

In addition, during the summer of 1996, we obtained comprehensive observations of two severe thunderstorms (10 and 12 July) in northeastern Colorado. Each lasted for over 4 h and featured intense radar reflectivities, significant hail, and total flash rates in excess of 30 min^{-1} at peak. However, the 10 July storm produced CG flash rates that generally were less than 1 min^{-1} during almost all of its lifetime. Nearly all CGs were of negative polarity. The 12 July storm produced similar CG flash rates during a significant portion of its lifetime. During this period the fraction of positive CGs was about 50%, but total CG flash rates were still about 1 min^{-1} or less. Some of the distinguishing characteristics of the 10 and 12 July storms—long life, intense radar reflectivities, significant production of hail, and high total flash rates—are similar to features of intense or severe storms that produce significant amounts of positive CG flashes. However, their CG lightning signature is similar to that of a nonsevere cell. The combination of enhanced IC flash rate and reduced CG flash rate may be analogous to the developing stage of an ordinary cell, but these features of the 10 and 12 July storms lasted for time periods greater than the typical total lifetime of an ordinary cell.

Thus, as CG lightning data become more available for ''nowcasting'' of severe weather, it is important to document and develop physical explanations for low CG rates (i.e., <1 min^{-1}) in certain intense, electrically active storms. In the next section, we review a possible mechanism to explain this phenomenon.

2. The elevated charge mechanism

MacGorman et al. (1989) studied ground flash rates relative to tornadic storm evolution for two storms that occurred in Oklahoma on 22 May 1981. Assuming the dipole model of thunderstorm charge structure [see Williams (1989) for a review of the dipole and tripole models of thunderstorm charge structure], with negatively charged particles at midlevels and positively charged particles at upper levels, they concluded that strong updrafts can suspend the negative charge center to higher altitudes than in ordinary nonsevere storms. According to MacGorman et al. (1989), three factors are relevant in this mechanism: 1) The strong updrafts quickly loft all but the largest particles to upper levels. 2) Strong updrafts do not allow hydrometeors to remain in a given layer as long as weaker updrafts so that particles have less time to grow, acquire charge, and separate charge. Thus there is less net negative or positive charge in a given layer. 3) Temperatures in a strong updraft core are higher relative to weaker cores, possibly causing the noninductive ice processes thought by many to be responsible for thunderstorm charging to occur at a higher altitude.

This elevated charge favors IC lightning over CG lightning due to the reduced average electric field between the negative charge center and ground caused by the increased distance between these two locations. In addition, a strong updraft core would cause regions of net negative and positive charge to be closer to one another, at least initially, according to MacGorman et al. (1989). These close charge regions would require less total charge to obtain the same average electric field between them. Additionally, the breakdown field for air decreases with height, so IC flashes should be enhanced due to the reduced breakdown potential in the region of elevated charge. This would limit total charge in these regions to lower magnitudes, another factor that would not favor CG flashes.

In addition, Krehbiel (1986) argued that the negative current that flows toward thunderstorm top (to produce a negative screening layer there) tends to make a storm more negative with time, making negative CG flashes more likely in the latter stages of a storm. If the upper positive charge region were reduced in magnitude as described above, it would tend to reduce this current and counteract the effect described by Krehbiel (1986). Hence, this is one more reason to expect fewer negative CG flashes in storms with intense updrafts.

Electric field measurements from balloon-borne soundings have shown that the standard dipole and tripole models of thunderstorm charge structure probably are incomplete (e.g., Marshall and Rust 1991; Marshall et al. 1995; Stolzenburg et al. 1998a–c). Stolzenburg et al. (1998c) suggested a new model. Within the updraft of a convective storm there are four charge layers of alternating polarity, with net positive charge in the lowest layer and net negative in the highest layer. Outside the updraft there are six charge regions of alternating polarity, again with positive in the lowest layer and negative in the highest.

Balloon studies do provide evidence for elevated

charge within strong updrafts. Rust et al. (1990) launched a balloon-borne electric field meter into a mesocyclone and found elevated negative charge on the order of 3–5 km higher in altitude compared to nonsevere storms. More recently, Marshall et al. (1995) inferred from 11 electric field soundings that charge may be elevated in strong updrafts. Finally, Stolzenburg et al. (1998a–c) reported findings from nearly 50 electric field soundings that clearly show that increasing the updraft speed elevates the entire charge structure within the updraft.

In terms of the elevated charge mechanism, it is possible to reconcile the dipole-based theoretical arguments of MacGorman et al. (1989) with the more complex model proposed by Stolzenburg et al. (1998c). It is generally believed that the main negative charge center is responsible for most of the negative CG lightning produced by a storm (e.g., Williams 1989). The Stolzenburg et al. (1998c) model supports the idea that this charge region will be elevated in a strong updraft, thereby reducing the overall electric field between that charge region and ground. The elevated charge structure also will be in a region of reduced breakdown potential due to the higher altitude. Stolzenburg et al. (1998a–c) provided some evidence, albeit weaker, that major charge centers are closer together within updrafts. The upper negative charge region in the Stolzenburg et al. (1998c) model is akin to the negative screening layer of Krehbiel (1986). Now, according to Stolzenburg et al. (1998c), outside the updraft the charge layers are not elevated. However, in intense storms enhanced IC flashing caused by the elevated updraft charge structure likely would limit total charge in both the updraft and nonupdraft regions, at least within the main negative and upper positive charge layers, so CGs may be less likely regardless. Thus, the elevated charge mechanism is still applicable within the Stolzenburg et al. (1998c) model.

Besides the balloon soundings, there have been other attempts to verify the elevated charge mechanism. MacGorman and Nielsen (1991) compared the Binger storm of MacGorman et al. (1989) to another severe storm that featured higher CG flash rates and concluded that the Binger storm was more intense overall, implying a stronger updraft. Ziegler and MacGorman (1994) used a kinematic retrieval that included electrification processes to model the Binger storm's charge structure and electric field. They found that the main negative charge region was elevated, as hypothesized earlier by MacGorman et al. (1989).

Based on these initial successes, it is clear that the elevated charge hypothesis deserves further testing and evaluation. Due to their relatively low production of CGs, the 10 and 12 July 1996 storms are excellent test cases to examine further the validity of this mechanism. We focus on detailed case studies of these storms below.

3. Overview of instrumentation

Phase A of the Stratosphere–Troposphere Experiments: Radiation, Aerosols, Ozone (STERAO-A) field project took place during the summer of 1996 over the plains of northeastern Colorado. The purpose of the project was to study trace gas production and transport by deep convection, especially nitrogen fixation by lightning. The project was physically centered around the CSU-CHILL multiparameter Doppler radar located near Greeley, Colorado. The radar was used to characterize the microphysical and kinematic structure of sampled storms. Also available was the Office National d'Etudes et de Recherches Aérospatiales (ONERA) VHF lightning interferometer (ITF), which mapped VHF emissions from lightning in three dimensions. Project participants had access to CG data from the National Lightning Detection Network (NLDN).

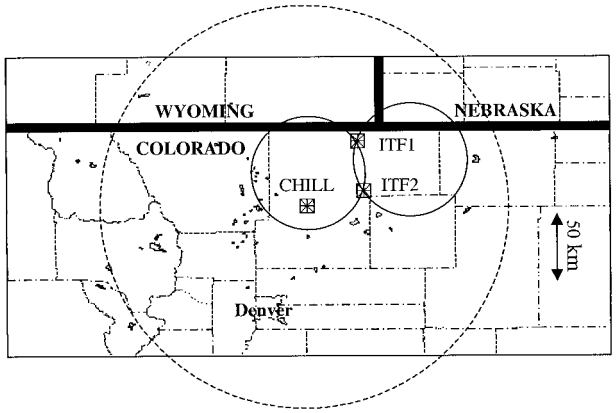

FIG. 1. Schematic map of the operational area of STERAO-A. Pictured are the locations of the CSU-CHILL radar and the VHF interferometer receiving stations (crossed squares). ITF1 refers to the combined azimuth and elevation receiving station, and ITF2 refers to the azimuth-only station The best-resolution lobes of the ITF are marked by the dark solid circles, and the 150-km range of the CSU-CHILL is marked by the dashed circle. Also shown are state and county lines, as well as major bodies of water and the approximate location of the city and county of Denver.

Figure 1 is a schematic map of the area in which the STERAO-A project took place. Included are the positions of the CSU-CHILL radar, which was configured with a maximum range of 150 km during STERAO-A, and the positions of the ITF receiving stations and the ITF's two resolution lobes, defined by location accuracies of 1–2 km or better.

The presence of data from both the CSU-CHILL radar and the ITF provided a unique dataset for which to study the relationships between convective storm microphysics and associated total lightning, specifically the phenomenon of low CG flash production by certain intense convective storms. We now present a description of the data and analysis methods.

a. CSU-CHILL radar facility

The CSU-CHILL radar is a dual-linearly polarized S-band Doppler radar with a wavelength of 11 cm and a beamwidth of 1°. The multiparameter variables mea-

sured by the CSU-CHILL radar include horizontal reflectivity (Z_h), radial velocity (V_r), differential reflectivity (Z_{DR}), linear depolarization ratio (LDR), correlation coefficient at zero lag (ρ_{hv}), and differential phase (Ψ_{DP}). These variables give information on the size, shape, orientation, thermodynamic phase, and radial velocity of hydrometeors in a bulk sense. For a thorough review of these variables, see Doviak and Zrnic (1993). In this study the main objective of the multiparameter radar data analysis was to detect and quantify the presence of hail and mixed-phase precipitation. Additionally, the horizontal reflectivity data were used to analyze basic storm structure and to relate to other observations.

A basic plan position indicator sector scanning strategy was used. Full volume coverage of storms with the preservation of adequate temporal resolution (~6 min or less) was the goal. Radar data were edited in postprocessing to remove clutter and other spurious echo. Differential phase was filtered to remove differential phase shift due to backscatter using the technique of Hubbert et al. (1993), which produced Φ_{DP}, the differential phase shift due to propagation. Specific differential phase, K_{DP}, was calculated via finite differencing the filtered Φ_{DP} field. All variables were interpolated to a Cartesian grid. The gridding scheme used a Cressman filter (Cressman 1959) with a variable radius of influence. Grid resolution for both case studies discussed in this paper was set at 1.0 km in both horizontal directions and 0.5 km in the vertical direction.

The multiparameter variables Z_{DR}, LDR, and ρ_{hv} are often corrupted in areas of strong elevational and azimuthal reflectivity gradients because of the effect of mismatched sidelobe patterns (Herzegh and Carbone 1984). The approach adopted in this work was to grid the data without editing for reflectivity gradients, and any analysis software that used Z_{DR}, LDR, and/or ρ_{hv} first calculated the local reflectivity gradient in Cartesian space. Then, based on a gradient threshold, a decision was made to include or exclude the particular data from the analysis. In this manner, sensitivity tests with different thresholds could be performed easily. Calculating the reflectivity gradient in Cartesian space is not strictly correct, however, as the natural coordinates of the radar are spherical, and gradients in spherical coordinate space are what cause the sidelobe contamination problem. But sidelobe contamination was not observed to be a serious issue with the two cases in this study, so significant effort to mitigate its effects was not required. This approximate approach utilized typical values for reflectivity thresholds varying from 10 to 20 dBZ km^{-1}. Little if any sensitivity to the choice of threshold was found.

Table 1 lists the multiparameter variable matrix employed in order to distinguish between different hydrometeor species in a bulk sense. This study employed Z_h, Z_{DR}, LDR, K_{DP}, and ρ_{hv} to determine regions of large (diameter $\geq$2 cm) hail, small ($<$2 cm) hail, large hail mixed with rain, small hail mixed with rain, and rain only. This matrix is identical to the one used by Carey and Rutledge (1998) and is applicable only when the environmental temperature is warmer than freezing.

TABLE 1. Hydrometer identification matrix, based on multiparameter radar data, used in this study to distinguish between bulk precipitation types below the freezing level; D is particle diameter.

Hydrometer type ($T \geq 0$°C)	Z_h (dBZ)	Z_{DR} (dB)	LDR (dB)	K_{DP} (° km^{-1})	ρ_{hv}
Small hail ($D < 2$ cm)	≥50	≤0.5	<−18	<0.5	>0.96
Small hail and rain	≥50	<1.0	−27 to −20	≥0.5	≤0.98
Large hail ($D \geq 2$ cm)	≥55	≤0.5	≥−18	<0.5	≤0.96
Large hail and rain	≥55	<1.0	≥−20	≥0.5	≤0.96
Rain	<60	>0.5	≤−27	≥0.5	≥0.97

This matrix was applied at each grid point where the temperature was above freezing to identify the main precipitation type present. These results were used to determine the area covered by each precipitation type at each grid level, as well as total volume of each precipitation type in the region of the storm that is below the altitude of the freezing level. These calculations were made for the entire storm complex, not any individual cell. While a cell-by-cell precipitation analysis may be preferable in some situations, in practice it would be difficult to do properly due to the possibility of the choice of analysis region geometry improperly influencing results.

b. NLDN

Recently, the NLDN was upgraded to its current combination of direction-finding and time-of-arrival technology. As a result of this upgrade, detection efficiencies in northeastern Colorado are projected to have improved to 90% or better with a median location accuracy of 0.5 km (Cummins et al. 1998).

An unexpected result of this upgrade was the inclusion of a previously undetected population of weak positive flashes. These discharges may not be true positive CGs; instead, many could be IC discharges that are being falsely identified as positive CGs. It has been suggested that some detected positive discharges with peak currents under 10 kA may be IC discharges (Cummins et al. 1998). Peak currents were estimated via the method recommended by Cummins et al. (1998). Five positive CGs with peak currents below this threshold were observed in the NLDN data from the 10 July 1996 storm, and seven positive CGs with a peak current below this threshold were observed in the 12 July 1996 storm. These flashes were not included in the CG flash rates and instead were counted as IC flashes.

c. ITF

The ONERA lightning ITF uses interferometric techniques to map VHF emissions from lightning in three dimensions (Laroche et al. 1994). Several researchers

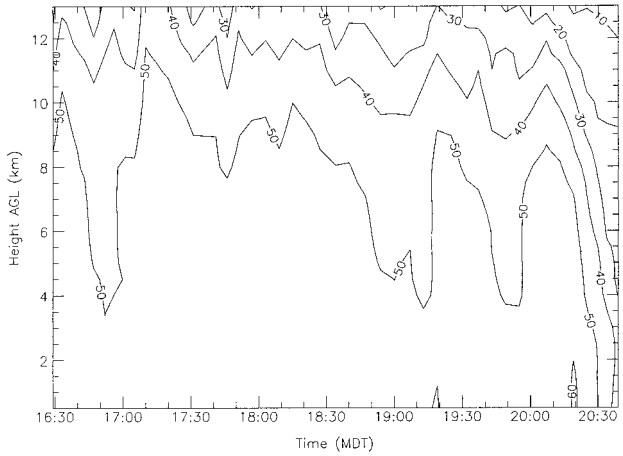

FIG. 2. Time–height cross section of peak radar reflectivity for the 10 Jul 1996 storm. Values are in dBZ.

(e.g., Warwick et al. 1979; Richard and Auffray 1985; Rhodes et al. 1994) have used interferometric lightning mapping in the past with good success. Our study used the ITF to compute total lightning flash rates, from which we subtracted NLDN-detected CGs to form the set of IC flashes, and to determine mean positions of flashes. Details of the ITF system and analysis approach are provided in the appendix.

4. Case studies

a. 10 July 1996

The storm of 10 July 1996 began as a multicellular line that developed in extreme southwestern Nebraska, near the town of Kimball, and then traveled south-southeast into Colorado. Late in its lifetime, the storm was composed of a single, intense cell.

Figure 2 shows a time–height cross section of maximum radar reflectivity for this storm. All cells were included in this analysis. The storm was very intense from the reflectivity data, with 30 dBZ often exceeding the top grid level at 13 km above ground level (AGL). (Radar data at higher levels were not gridded as storm-top information was not necessary for the purposes of this paper.) For much of this storm's lifetime, 50 dBZ extended above 8 km AGL, dropping to lower levels only occasionally and then only for a short duration, except at the end when the storm collapsed totally.

Five-minute IC flash rates from the ITF and 5-min NLDN CG rates were calculated for this storm complex. These time series are shown in Fig. 3, with flash rates plotted at the end of their respective time periods. Except for a few times, the storm was located completely within the eastern lobe of the ITF. During the period 1800–1850 mountain daylight time (MDT) there was significant redevelopment of the storm on its northwest flank, which extended partially beyond the northern end of the eastern ITF lobe. Thus, IC flash rates are likely to be underestimated during this time.

The entire storm complex, throughout its lifetime, produced relatively few CGs (and the overwhelming majority of these were negative polarity; hence, CG rates were not separated into positive and negative CG components). The peak CG flash rate was 8 in a 5-min period (near 1810 MDT), fairly low when compared to mean peak or even average CG flash rates for multicell storms (e.g., Uman 1987, p. 49). Apart from this time, CG rates were extremely low, well under 1 min^{-1}. Throughout the storm's lifetime there were several time periods, lasting 10 to almost 30 min, when there were no CGs detected by the NLDN. The most striking examples of these are the periods 1645–1710 and 1925–1945 MDT.

This second time period (1925–1945 MDT) coincided with a maximum in the IC flash rate, with flash rates over 30 min^{-1}. Between 1825 and 1915 MDT, IC flash rates were steady, averaging approximately 15 min^{-1} with only small deviations from this rate. Before 1825, IC rates were more variable. After the IC flash rates reached their maximum values near 1925, they remained steady for another 20 min, underwent another major fluctuation, and then decreased rapidly as the final cell in the storm complex (based on radar observations) collapsed.

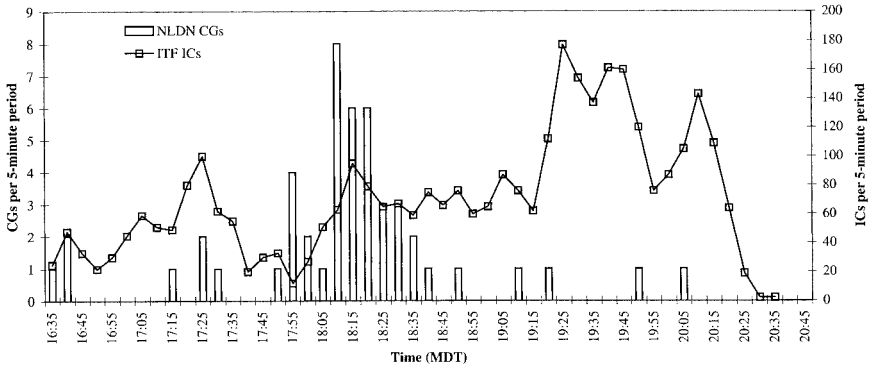

FIG. 3. The 5-min NLDN CG rates and 5-min ITF IC rates for the 10 Jul 1996 storm. Data points are plotted at the end of each 5-min period.

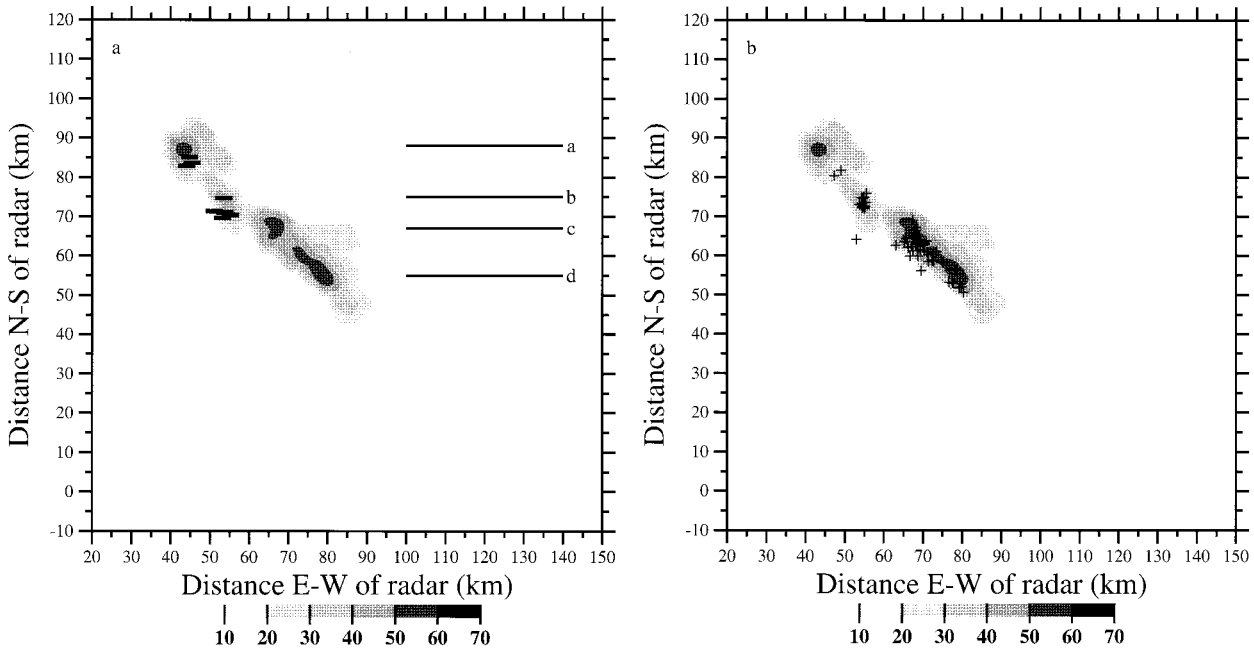

FIG. 4. (a) Horizontal cross section of radar reflectivity (dBZ) at 0.5 km AGL for the 1809 MDT radar volume. Also shown are ground-strike locations of all NLDN-detected CG lightning that occurred during the period 1805–1810 MDT. Negative CGs are marked with a minus sign, and positive CGs are marked with a plus sign. The lines marked a–d correspond to the respective vertical cross sections in Fig. 5. (b) Same as (a) except for mean positions of IC flashes, marked by the small crosses.

Figure 4a shows NLDN CG ground strike locations overlaying low-level radar reflectivity data for the 1809 MDT volume scan. This is around the time of peak CG production by this storm. The CGs shown are those that occurred between 1805 and 1810 MDT (i.e., flashes included in the 1810 flash rate in Fig. 3). The northernmost cells, which featured lower peak radar reflectivities at 0.5 km AGL, were producing the most CGs during this time. The southernmost cells produced no CGs during this time period, but featured substantial radar reflectivities (>50 dBZ).

Figure 4b presents the same analysis, but for IC flashes. The most ICs were associated with the stronger cells (in terms of low-level reflectivity), while fewer ICs were associated with the weaker northern cells. However, at this time the northernmost cell was partially outside the ITF lobe, so not all IC flashes produced by this cell were detected.

To gain a better sense of the vertical extent of each cell around this time, vertical cross sections of radar reflectivity for the 1809 MDT volume taken along various distances north of the CHILL radar are shown in Fig. 5. Figure 5a is for the northernmost cell in the line from Fig. 4, Fig. 5b is for the next cell to the south, and so on through Fig. 5d, which is for the southernmost cell along the line. The vertical extents of the 50-dBZ contour for the two southernmost cells, the cells which produced very few CGs around this time, are much greater than the northern two cells, which accounted for most of the CGs. The low-CG cells show 50 dBZ up to 6 km AGL or more, whereas the CG-producing cells either lack 50 dBZ altogether (as in Fig. 5b), or this reflectivity contour extends to a significantly lower altitude (4 km in Fig. 5a). This is strong evidence that the cells producing the fewest CGs were much more intense than the cells producing the most CGs and that the internal structures of the two types of cells were different. Specifically, the most hail (based on multiparameter radar data) was associated with the low-CG cells. Throughout the lifetime of this storm, very few CGs but most of the ICs can be attributed to the most intense cell(s) at any specific time.

Storm volumes below the altitude of the freezing level (3.29 km AGL on this day) occupied by various hydrometeor types were calculated for each radar volume (using multiparameter variables; cf. Table 1). The sum of storm volumes (below the altitude of the freezing level) containing small hail or small hail mixed with rain is indicated in Fig. 6. For comparison, the volumes of echo below the freezing level equal to or exceeding 30 dBZ and 50 dBZ, respectively, also are shown. The precipitation identification matrix detected little if any large hail. This is confirmed by examining the ρ_{hv} fields. With relatively high values typically ranging from 0.97 to 0.99 throughout the case, ρ_{hv} did not suggest any non-Rayleigh scattering that would have been associated with the presence of large hail. Note that these values are for the entire storm *complex,* not any individual cell. At 1751 MDT and again at 1907 MDT radar coverage was extended to include new cells forming on the northwest end of the line. Thus, trends around these times are somewhat compromised.

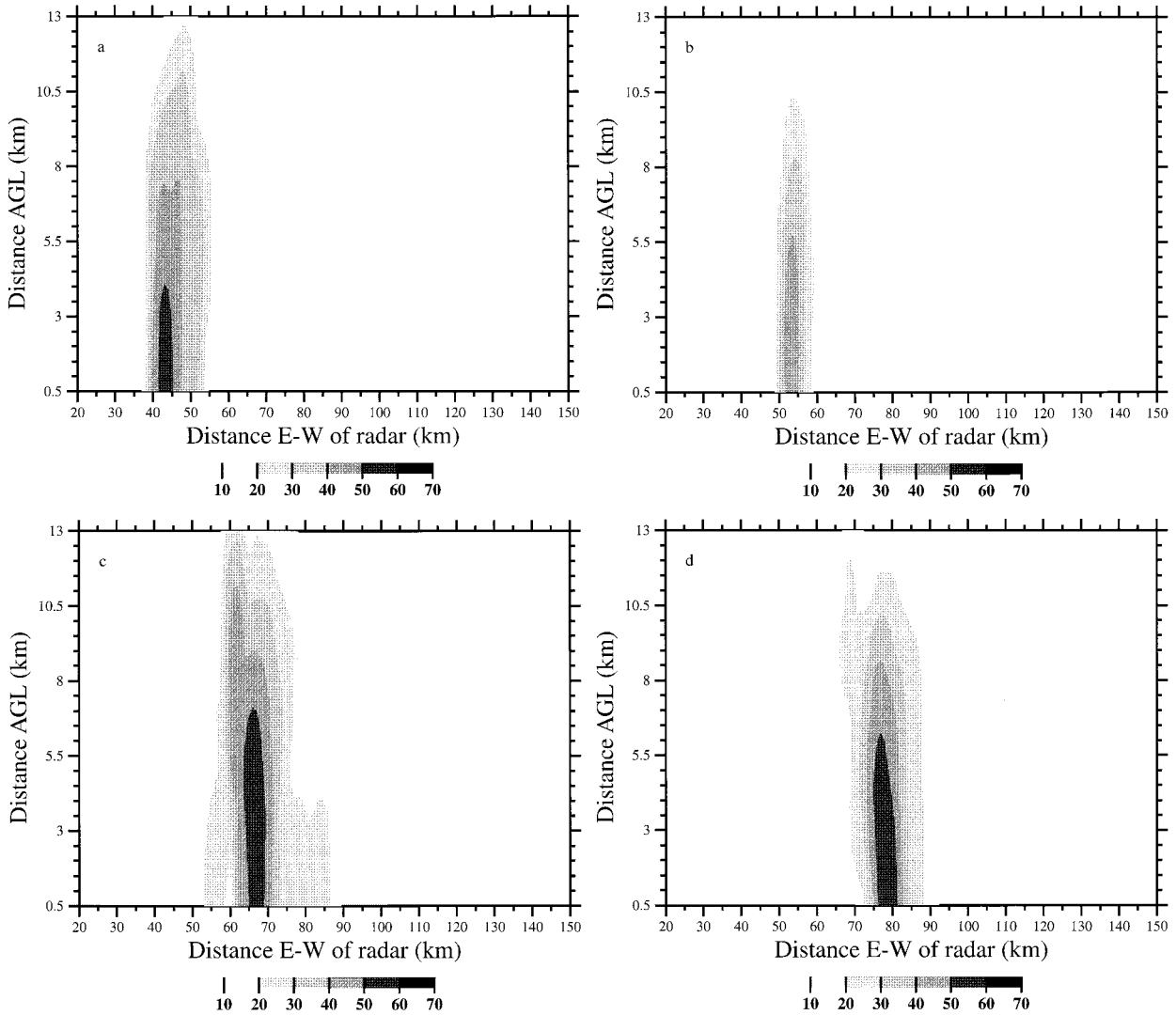

FIG. 5. (a) Vertical cross sections of radar reflectivity (dBZ) at 88 km north of the CHILL radar for the 1809 MDT volume scan. (b) Same as (a) except at 75 km north of CHILL. (c) Same as (b) except at 67 km north of CHILL. (d) Same as (c) except at 55 km north of CHILL.

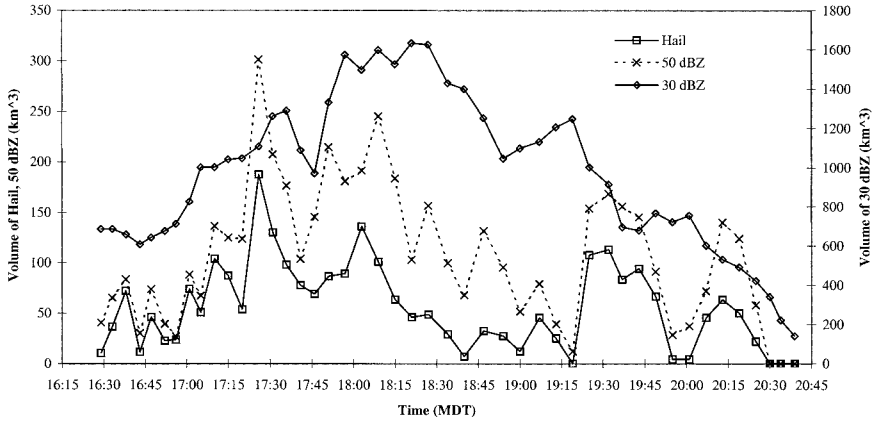

FIG. 6. Time history of the radar-inferred volume of small hail and small hail mixed with rain below the freezing level for the 10 Jul 1996 storm. Also shown are the time histories of the volumes (below the freezing level) of echo equal to or exceeding 30 and 50 dBZ, respectively.

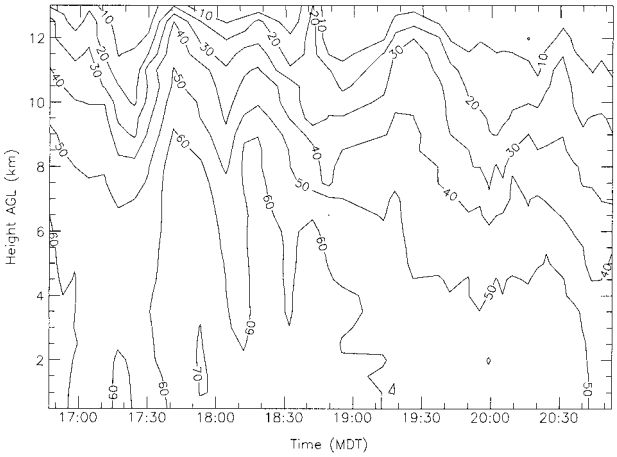

FIG. 7. Time–height cross section of peak radar reflectivity for the 12 Jul 1996 storm. Values are in dBZ. Times with insufficient data at lower levels are completely blank, and times with insufficient data at upper levels lack contouring at those levels.

According to Fig. 6, significant amounts of hail were produced throughout the storm's lifetime, although such production was variable. At peak there were slightly less than 200 km^3 of storm that contained small hail, whether alone or mixed with rain (compared to 1400 km^3 for the storm volume equal to or exceeding 30 dBZ). Throughout the storm's lifetime hail volume was a significant fraction of the volume containing 50 dBZ or greater. When hail production dropped toward zero, it did not stay that way for long, generally returning to higher values within the next 10 min, except at the end of the storm's lifetime. This suggests that vigorous new convection, and hence hail production at upper levels, was occurring even as older cells matured and collapsed.

b. 12 July 1996

The storm on 12 July 1996 developed in extreme southern Wyoming between the cities of Laramie and Cheyenne. It then moved to the southeast toward the CSU-CHILL radar, passing just east of the radar site, and continued moving to the southeast away from the radar. When radar coverage began around 1600 MDT the storm complex was large, but weak and multicellular. Around 1715 MDT a very intense cell developed on the southwest side. Sector sweeps suitable for multiparameter studies started around 1645 MDT. Throughout its lifetime, the storm complex remained multicellular, usually with one cell dominating much of the reflectivity pattern, though there also were other intense cells at times. Around 1900 MDT the storm complex weakened, featuring lower peak radar reflectivities, as well as a less pronounced vertical reflectivity structure, though it continued to persist in some form for another 2 h.

Figure 7 shows a time–height cross section of maximum radar reflectivity for this storm. All cells were included in this analysis. Unfortunately, because this storm came so close to the radar, we sometimes lacked sufficient data at several levels, especially near storm top, to make completely accurate estimates of the peak radar reflectivities at those levels. This generally occurred as scan coverage was compromised in order to keep temporal resolution adequate, mostly during the period from 1830 to 1930 MDT, and estimates of maximum radar reflectivity at upper levels are likely to be underestimates between these times. Radar volumes consisting of only a few low-level sweeps are not included in the time–height analysis shown in Fig. 7. During the early stage of sector coverage, the storm was very intense, with 60 dBZ above 8 km AGL around 1750 MDT. After 1900 MDT the storm appeared significantly weaker, with 50 dBZ up to only 4–5 km AGL.

Figure 8 shows 5-min CG lightning rates as functions of time for the entire storm complex, separated into positive and negative CG components, as well as 5-min ITF-determined IC flash rates. The lifetime of this storm can be separated into two relatively distinct phases, as defined by the CG flash rate. In the first phase (prior to 1900 MDT), CG flash rates for either polarity were low,

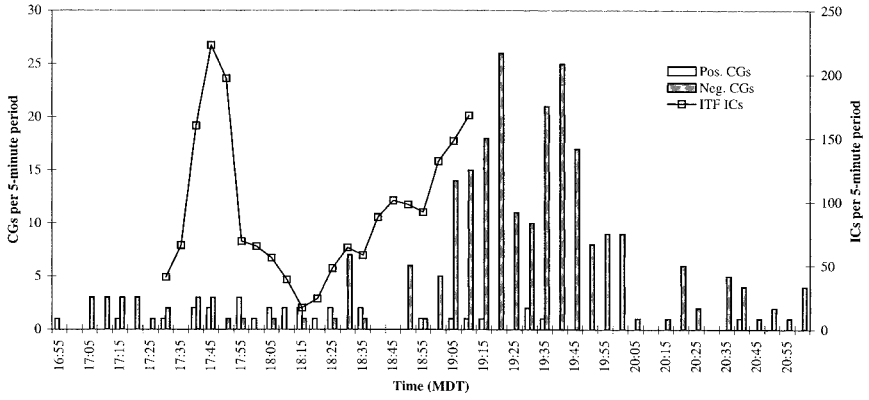

FIG. 8. The 5-min NLDN CG rates (separated by positive and negative CGs) and 5-min ITF IC rates for the 12 Jul 1996 storm. Data points are plotted at the end of each 5-min period.

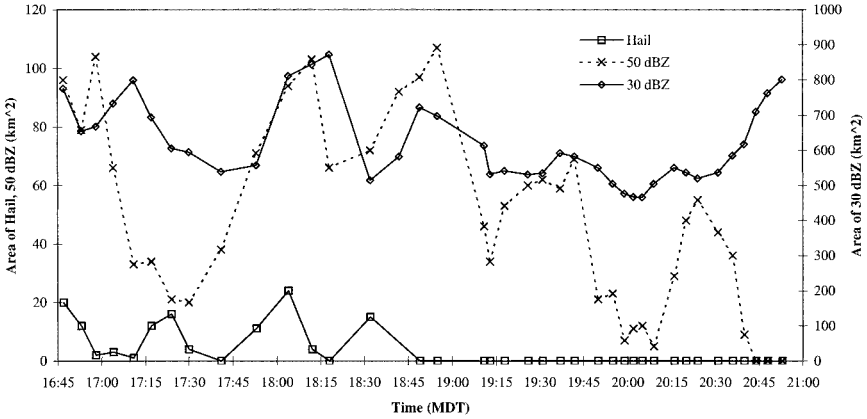

FIG. 9. Time history of the radar-inferred area at 0.5 km AGL of small hail and small hail mixed with rain for the 12 Jul 1996 storm. Also shown are the time histories of the areas (at 0.5 km AGL) of echo equal to or exceeding 30 and 50 dB*Z*, respectively.

typically less than 1 min^{-1}. During this phase a large percentage of the CGs were of positive polarity, about 50% (although total CG flash rates were low). However, after 1900 MDT, positive CG rates remained similar for less than an hour and then declined to zero until near the end of radar coverage. Negative CG flash rates rose sharply, peaking around 5 min^{-1} at 1920 MDT and again at 1940 MDT, then decreased to more modest values late in the lifetime of the storm complex.

This particular storm complex was not ideally situated in relation to the ITF lobes, which can result in compromised flash detection near the lobe boundaries. After 1800 MDT, the eastern extent crossed from the western lobe into the eastern lobe. However, until 1910 MDT, the main cell cores were well placed in either ITF lobe, with the main western cores within the western lobe and the main eastern cores in the eastern lobe, with only weak echo in the vicinity of the ITF baseline. The IC rates that were calculated are likely to be underestimates after 1800 MDT. However the main cores, which were producing the vast majority of ICs prior to this time period, were still well positioned in the ITF lobes. Thus, IC flashes in these cores were detected and storm complex IC flash rates are not likely to be significantly compromised. After 1910 MDT, the main storm began moving out of the southern boundaries of both lobes, so although flashes still were being detected in part, flash rate calculations were not done for later times. They also were not computed for times prior to 1730 MDT when the northern part of the storm complex extended beyond the northern boundary of the ITF domain.

For the time period that data were available, ITF IC flash rates were extremely variable, ranging from over 40 min^{-1} to less than 10 min^{-1}. However, from 1813 MDT to 1822 MDT, VHF sources detected by the ITF were very scattered and erratic, and did not appear normal. The transitions into and out of this regime were very abrupt. It is likely that the ITF was not functioning properly during this time, so IC flash rates probably were underestimated during this time period.

Because this storm came so close to the radar it was difficult to obtain adequate upper-level data to make accurate estimates of the total volume of each precipitation type, even below the altitude of the freezing level. Instead, we show the time history of the area of small hail and small hail mixed with rain at 0.5 km AGL for the entire storm complex in Fig. 9. Radar volumes consisting of only a few low-level sweeps are included in this analysis, though they were not included in Fig. 7. For comparison, the areas of echo at 0.5 km AGL equal to or exceeding 30 and 50 dB*Z*, respectively, also are shown. Around 1855 MDT the radar scanning sector was not large enough to include all of a new cell developing on the southern portion of the storm, so values around this time probably are slight underestimates, in particular the 30-dB*Z* echo contour area.

As with the 10 July storm, the presence of significant quantities of large hail as determined by the radar was negligible, although a few spotter reports of 2-cm-diameter and larger hail do exist for both the 10 and 12 July storms. Based on the multiparameter radar data, almost all hail were smaller than 2 cm throughout the analyzed periods of both storms, so these spotter-reported hailstone sizes probably lay on the extreme end of the hail size spectra for these storms.

There is a significant decrease in hail area near 1900 MDT. Before this time, the hail area was significant (relative to 50-dB*Z* echo contour coverage), though of a pulsing nature related to individual cell growth and decay. After this time, the hail area was essentially zero. This change correlates well with the increase in negative CG rates in the storm complex.

In Figs. 8 and 9 note that around 1804 MDT, CG flash rates were low, and storm complex hail area was near its maximum. Figure 10a depicts a horizontal cross section of reflectivity at 0.5 km AGL at 1804 MDT along

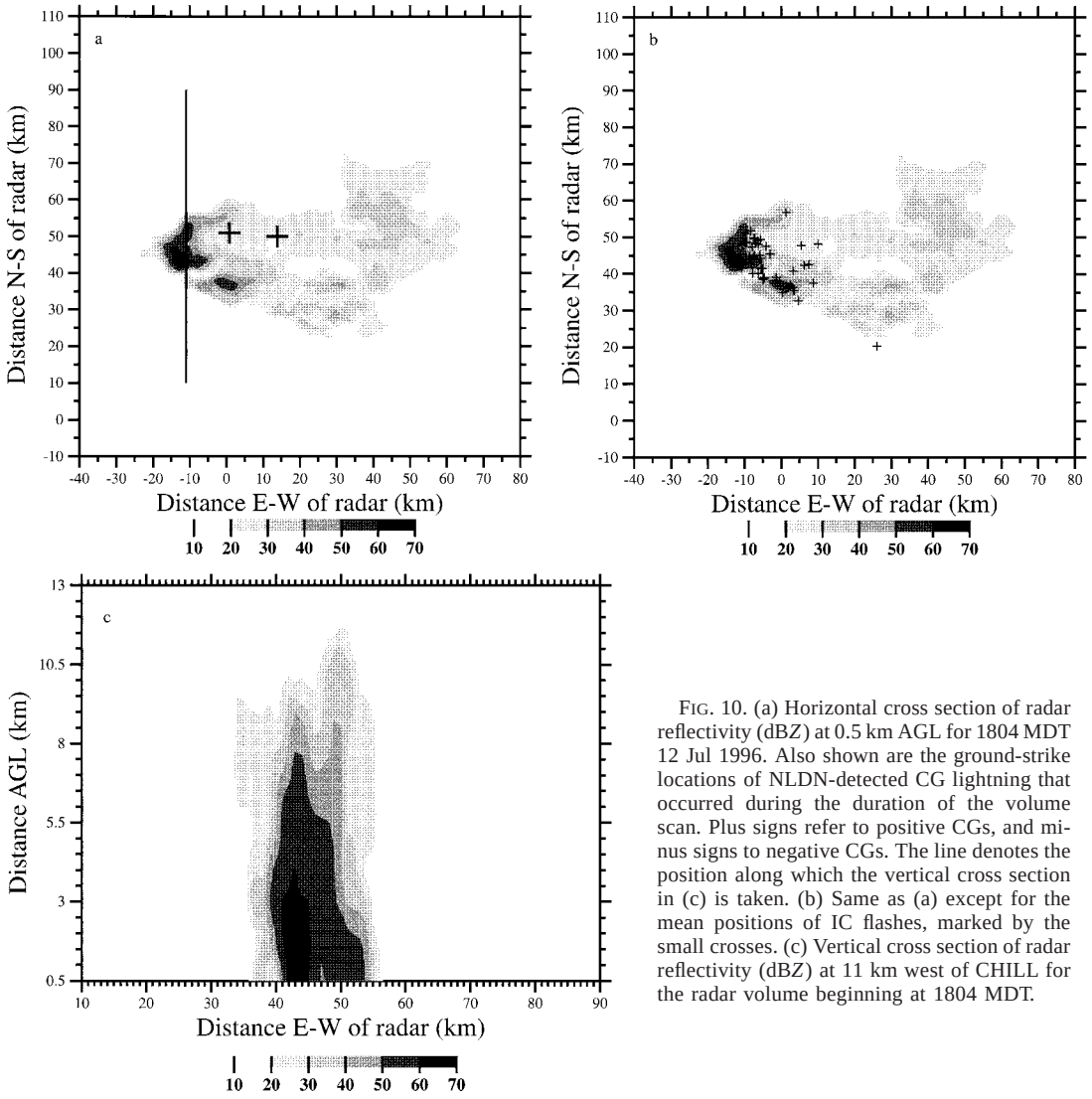

FIG. 10. (a) Horizontal cross section of radar reflectivity (dBZ) at 0.5 km AGL for 1804 MDT 12 Jul 1996. Also shown are the ground-strike locations of NLDN-detected CG lightning that occurred during the duration of the volume scan. Plus signs refer to positive CGs, and minus signs to negative CGs. The line denotes the position along which the vertical cross section in (c) is taken. (b) Same as (a) except for the mean positions of IC flashes, marked by the small crosses. (c) Vertical cross section of radar reflectivity (dBZ) at 11 km west of CHILL for the radar volume beginning at 1804 MDT.

with ground-strike locations and polarities of NLDN-detected CG lightning that occurred during this volume scan (~6 min in duration). Figure 10b shows the same analysis except for IC lightning. A vertical cross section of radar reflectivity 11 km west of CHILL at the same time is shown in Fig. 10c. Based on this cross section, the cell appears intense, with the 30-dBZ contour extending to 11 km AGL, and the 50-dBZ contour extending to 7.5 km AGL.

Figure 11a shows a horizontal cross section of reflectivity at 0.5 km AGL for the radar volume at 1937 MDT. Also shown are the ground-strike positions and polarities of NLDN-detected CG lightning that occurred during this volume (~6 min). At this time the negative CG rates were near their peak, and the storm was divided into two main regions. Likewise, CG lightning around this time was divided nearly equally between the two major cell complexes. Because the storm extended well outside the ITF lobes at this time, flash detection by the ITF was compromised so IC flashes are not shown for this volume.

Figures 11b and 11c show vertical cross sections of reflectivity at this time at 24 km east of CHILL and 56 km east of CHILL, respectively. These two cross sections bisect the approximate centers of the major cells. Comparing these vertical cross sections with Fig. 10b, it is apparent that cell structure is radically different between the two times. The 30-dBZ contours at 1937 MDT extend to only 9.5 km AGL for either cell complex. The 50-dBZ contours extend to 4 km AGL or less. There is no region of 60 dBZ and greater reflectivity as there was at 1804 MDT, when the 60-dBZ contour extended to 4 km AGL.

Overall, the storm complex at 1937 MDT appears much less intense, based on both horizontal and vertical reflectivity structure, compared to the storm at 1804

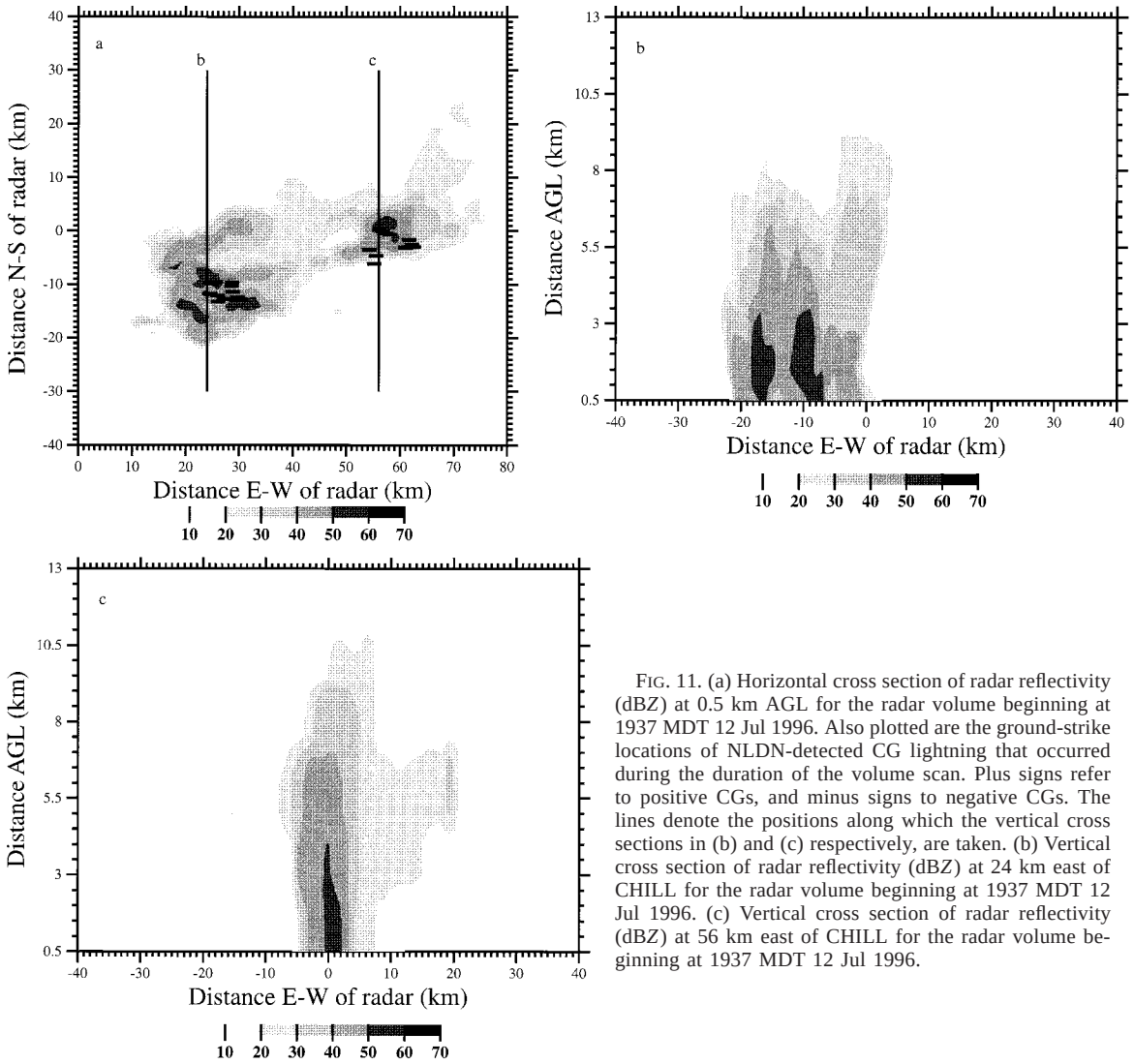

FIG. 11. (a) Horizontal cross section of radar reflectivity (dBZ) at 0.5 km AGL for the radar volume beginning at 1937 MDT 12 Jul 1996. Also plotted are the ground-strike locations of NLDN-detected CG lightning that occurred during the duration of the volume scan. Plus signs refer to positive CGs, and minus signs to negative CGs. The lines denote the positions along which the vertical cross sections in (b) and (c) respectively, are taken. (b) Vertical cross section of radar reflectivity (dBZ) at 24 km east of CHILL for the radar volume beginning at 1937 MDT 12 Jul 1996. (c) Vertical cross section of radar reflectivity (dBZ) at 56 km east of CHILL for the radar volume beginning at 1937 MDT 12 Jul 1996.

MDT. Thus, marked differences in storm intensity between the two times correspond well to the marked differences in CG rates. This is further confirmation of what was seen in the hail data. Significant hail area, even though it underwent major fluctuations, corresponded to low CG flash rates, but very low to negligible hail area corresponded to significant numbers of negative CGs. The abrupt increase and largest value of IC flash rates (around 1800 MDT) occurred when the storm was intensifying rapidly. For this storm at least, storm intensity, as determined by the existence of hail and the maximum heights of the 30- and 50-dBZ reflectivity contours, was inversely correlated with negative CG lightning. Intensification was correlated with IC lightning.

5. Discussion and conclusions

The storm of 10 July 1996 underwent a major transition approximately halfway through the observational period, evolving from a multicellular line to an intense unicellular storm. Throughout this storm's lifetime CG flash rates were extremely low, usually well under 1 min^{-1}. During the peak CG flash rate period flashes typically were associated with less intense (in terms of peak radar reflectivity and vertical reflectivity structure) cells along the line, while the most intense cells were associated with the bulk of the IC flashes. During the storm's intense unicellular stage, CG production was zero, while IC flash rates peaked near 35 min^{-1}. Hail was inferred from multiparameter radar to be present throughout the storm's lifetime.

The storm of 12 July 1996 underwent a major transition from an intense, hail-producing multicellular storm to a weaker multicellular rainstorm with little if any hail production. Before this transition, CG flash rates were low (for both positive and negative polarity flashes), averaging less than 1 min^{-1}. After the transition, negative CG flash rates rose significantly, peaking

at 5 min^{-1}. The major cells before this transition had greater peak reflectivity and stronger vertical reflectivity structures than the major cells after the transition.

Some interesting common features are worth noting for these storms. One is that when hail was produced by either storm, even if such production underwent significant pulsing, CG flash rates were low. Another common feature is that CGs most often were associated with weaker cells, in terms of the vertical structure of radar reflectivity and the lack of hail. The most intense cells typically were associated with the bulk of the IC production. A final common aspect is that, especially when CG flash rates were low, these storms did not seem to follow the typical pattern of CG flash rates peaking when significant precipitation reached the ground. Cloud-to-ground flash rates remained low regardless of whether the most intense cells were developing or collapsing. Only when hail production largely was terminated, on 12 July, did CG flash rates increase. On 10 July, when hail production was terminated the storm itself collapsed, and no final burst of CGs occurred.

These observations are consistent with the elevated charge hypothesis of MacGorman et al. (1989). In cells producing the most CGs, the available proxy data (vertical structure of radar reflectivity and the presence of hail as inferred by multiparameter radar) imply weaker updrafts than in cells producing little or no CGs. In the cells that produced the most CGs, the vertical reflectivity structure was weaker, in that high radar reflectivity contours either did not exist or extended to lower altitudes than the more intense cells, which produced the fewest CGs. Intense updrafts are needed for hail production to occur. Thus, if there is little or no hail being produced, as during the latter half of the 12 July storm's lifetime, this implies weaker updrafts, on average, than a hail-producing storm. Note that this argument does not apply to a low-precipitation supercell, but the 12 July 1996 storm did not fit this category.

However, the elevated charge hypothesis does not explain why CG flash rates remain low even as cells collapse in these two storms. High IC flash rates may be the reason for this. MacGorman et al. (1989) postulated that the reduced separation between the main charge regions caused by an intense updraft would tend to limit the total charge contained in those regions due to enhanced IC discharging. High IC flash rates could effectively neutralize the main negative charge region, which already may have been reduced in magnitude, before it descended. Then CGs may be less likely to occur. This simple hypothesis, though consistent with the available data, obviously requires more thorough examination from both the observational and modeling perspectives in order to determine its validity.

It is not clear, based on the elevated charge mechanism, what distinguishes these low-CG intense storms from other intense or severe storms that may exhibit relatively high CG flash rates, especially high positive CG flash rates (e.g., Carey and Rutledge 1998). Positive CG storms and the storms studied in this paper tend to share a number of characteristics, such as intense vertical development, significant hail production, high IC flash rates, and a relative dearth of negative CG lightning. The only major way in which they differ is that the 10 and 12 July storm did not produce significant positive CG lightning. Further research on both types of storms is required.

Before concluding, we feel it is appropriate to discuss some other possible mechanisms that may explain the lightning behavior in 10 and 12 July. One could be the disruption of charging caused by the presence of wet growth hail. Saunders et al. (1991) and Saunders and Brooks (1992) argued that, based on noninductive charging theory, charge separation is ineffective when rimed ice particles enter the wet growth mode. This could disrupt the production of a lower positive charge region, which may inhibit negative CG flash rates (e.g., Williams 1989). However, based on the radar data, significant amounts of wet growth ice above the freezing level, as inferred from enhanced LDR values collocated with high radar reflectivities, were not observed during most or all of these two storms' lifetimes. Therefore, we do not believe wet growth was significant in these storms.

Another mechanism is that for intense storms with high precipitation rates, the electrical current associated with charged precipitation (precipitation current, J_P) may be large enough to offset charge carried to ground by the CG lightning current (J_L). Estimates of J_p (e.g., Christian et al. 1980; Marshall and Winn 1982; Marshall 1993) and J_L (Livingston and Krider 1978) suggest that J_P could become large relative to J_L provided precipitation rates are high. However, during the 10 July 1996 storm peak rain rates typically were low to moderate (often well under 60 mm h^{-1}) and during the 12 July 1996 storm peak rain rates typically were high (usually >60 mm h^{-1} and often >100 mm h^{-1}). Moreover, rain rates were high throughout the 12 July case, not just during the time it produced few CGs. Given these contradictions, this mechanism appears to be a poor explanation for observations, unless significant charge were carried by the hail. However, this is unlikely due to the typically low number concentration of hail (Cheng and English 1983) relative to graupel, which would be expected to melt into rain below the altitude of the freezing level.

In summary, this study provides additional documentation of the phenomenon of low negative CG production (<1 min^{-1}) but high IC flash rates (>30 min^{-1}) in certain intense thunderstorms. The available data tend to support the elevated charge mechanism of McGorman et al. (1989). From a forecasting perspective, this study establishes that low production of negative CGs can be correlated to the production of significant quantities of hail, high IC flash rates, and strong updrafts. This suggests that some intense or severe storms may be identifiable by relatively low negative CG production.

Acknowledgments. For their help in obtaining, examining, and interpreting the data used in this study, the authors wish to thank Patrice Blanchet of ONERA; the CSU-CHILL radar staff of Pat Kennedy, Dave Brunkow, Bob Bowie, and Ken Pattison; and the NASA Marshall Space Flight Center. This work was supported under National Science Foundation Grant ATM-9321361. Partial support for the ONERA interferometer was provided by the NASA Atmospheric Effects of Aviation Program and the NOAA Aeronomy Lab. The National Center for Atmospheric Research is partially funded by the National Science Foundation.

APPENDIX

Analysis of VHF Lightning Interferometer Data

VHF lightning interferometers primarily detect emissions from negative discharge processes (Rhodes et al. 1994) because they emit more VHF radiation than positive discharges. Thus the ONERA ITF, which receives in the 110–118-MHz band, detects three basic types of discharges: the negative leader, the recoil streamer, and the spider discharge (Laroche et al. 1994). See Uman (1987, chapters 5 and 13) for a detailed review of the first two types of discharges. Spider discharges are discussed in Mazur et al. (1998). Recoil streamers and spider discharges generally are associated with IC lightning, whereas negative leaders are associated with both CG and IC lightning. It is important to note that positive leaders, return strokes, and continuing current are not readily seen by the ITF.

During postprocessing of the data using software developed by ONERA, flashes were identified using criteria based on current knowledge of the various VHF-emitting lightning discharge processes (P. Laroche 1997, personal communication). The criteria govern how the software groups individual localizations (i.e., single VHF sources) into VHF radiation bursts and how it groups these bursts into separate flashes. From these total flash rates, CGs detected by the NLDN are subtracted to form the set of IC flashes.

It has been noted by the authors that when a storm was close to the north–south baseline of the two interferometer antennas, say, for example, the storm was near a lobe's northern edge, azimuthal resolution by the station (ITF2 in Fig. 1) was poor and source positions would be dispersed radially relative to the northern ITF station (ITF1). This problem occurred during the period before 1930 MDT on 10 July 1996 and it also occurred during 12 July 1996, but outside the IC flash rate analysis domain. This radial dispersion could affect mean positions of some flashes slightly but is not believed to impact flash rates, nor the overall placement of flashes relative to the radar structure.

Approximately one-third of flashes identified by the ITF for the 10 and 12 July 1996 storms lasted less than 1 ms in duration, with many of these lasting only as long as the ITF's fastest time resolution, 23 μs. The rest of the IC flashes identified by the ITF were roughly lognormally distributed around 250 ms. The average lightning flash generally is considered to last on the order of hundreds of milliseconds, so these populations of ''submilliseconds'' or ''short-duration'' flashes last on the order of the duration of individual discharges within a longer flash (Uman 1987, p. 124). These submillisecond ITF flashes probably are individual short-duration IC flashes, but their nature is not understood fully.

These short-duration flashes are worth studying in their own right, but they were not the focus of this study, which is interested in presenting IC flash rates that can be effectively compared to those presented in past lightning studies (e.g., Carey and Rutledge 1998) that did not have data on short-duration discharges. During analysis it was observed that removing the submillisecond flashes from consideration did not change IC flash rate *trends* significantly, though absolute flash rates did change. Given the use of IC data in this study, this change should have little impact on results. Therefore, the IC flash rates presented in this paper do not include flashes lasting less than 1 ms.

REFERENCES

Billingsley, D. B., and M. I. Biggerstaff, 1994: Evolution of cloud-to-ground lightning characteristics in the convective region of a mesoscale convective region. Preprints, *Fifth Symp. on Global Change Studies: Symp. on Global Electrical Circuit, Global Change, and the Meteorological Applications of Lightning,* Nashville, TN, Amer. Meteor. Soc., 340–344.

Branick, M. L., and C. A. Doswell III, 1992: An observation of the relationship between supercell structure and lightning ground-strike polarity. *Wea. Forecasting,* **7,** 143–149.

Carey, L. D., and S. A. Rutledge, 1996: A multiparameter radar case study of the microphysical and kinematic evolution of a lightning producing storm. *Meteor. Atmos. Phys.,* **59,** 33–64.

——, and ——, 1998: Electrical and multiparameter radar observations of a severe hailstorm. *J. Geophys. Res.,* **103,** 13 979–14 000.

Cheng, L., and M. English, 1983: A relationship between hailstone concentration and size. *J. Atmos. Sci.,* **40,** 204–213.

Christian, H. J., C. R. Homes, J. W. Bullock, W. Gaskell, A. J. Illingworth, and J. Latham, 1980: Airborne and ground-based studies of thunderstorms in the vicinity of Langmuir Laboratory. *Quart. J. Roy. Meteor. Soc.,* **106,** 159–174.

Cressman, G. P., 1959: An operational objective analysis system. *Mon. Wea. Rev.,* **87,** 367–374.

Cummins, K. L., M. J. Murphy, E. A. Bardo, W. L. Hiscox, R. B. Pyle, and A. E. Pifer, 1998: A combined TOA/MDF technology upgrade of the U.S. National Lightning Detection Network. *J. Geophys. Res.,* **103,** 9035–9044.

Curran, E. B., and W. D. Rust, 1992: Positive ground flashes produced by low-precipitation thunderstorms in Oklahoma on 26 April 1984. *Mon. Wea. Rev.,* **120,** 544–553.

Doviak, R. J., and D. S. Zrnic, 1993: *Doppler Radar and Weather Observations.* 2d. ed. Academic Press, 562 pp.

Fuquay, D. M., 1982: Positive cloud-to-ground lightning in summer thunderstorms. *J. Geophys. Res.,* **87,** 7131–7140.

Goodman, S. J., D. E. Buechler, P. D. Wright, and W. D. Rust, 1988: Lightning and precipitation history of a microburst-producing storm. *Geophys. Res. Lett.,* **15,** 1185–1188.

——, ——, ——, ——, and K. E. Nielsen, 1989: Polarization radar and electrical observations of microburst producing storms during COHMEX. Preprints, *24th Conf. on Radar Meteorology*, Tallahassee, FL, Amer. Meteor. Soc., 190–112.

Herzegh, P. H., and R. E. Carbone, 1984: The influence of antenna illumination function characteristics on differential reflectivity measurements. Preprints, *22d Conf. on Radar Meteorology*, Zurich, Switzerland, Amer. Meteor. Soc., 281–286.

Hubbert, J., V. Chandrasekar, V. N. Bringi, and P. Meischner, 1993: Processing and interpretation of coherent dual-polarized radar measurements. *J. Atmos. Oceanic Technol.,* **10,** 155–164.

Knapp, D. I., 1994: Using cloud-to-ground lightning data to identify tornadic thunderstorm signatures and nowcast severe weather. *Natl. Wea. Dig.*, **19,** 35–42.

Krehbiel, P. R., 1986: The electrical structure of thunderstorms. *The Earth's Electrical Environment*, E. P. Krider and R. G. Roble, Eds., National Academy Press, 90–113.

Laroche, P., A. Bondiou, P. Blanchet, J. Pigere, M. Weber, and B. Boldi, 1994: 3D mapping of lightning discharge within storms. ONERA Publ. 1994-186, 11 pp.

Larson, H. R., and E. J. Stansbury, 1974: Association of lightning flashes with precipitation cores extending to height 7 km. *J. Atmos. Terr. Phys.*, **36,** 1547–1553.

Livingston, J. M., and E. P. Krider, 1978: Electric fields produced by Florida thunderstorms. *J. Geophys. Res.*, **83,** 385–401.

MacGorman, D. R., and K. E. Nielsen, 1991: Cloud-to-ground lightning in a tornadic storm on 8 May 1996. *Mon. Wea. Rev.*, **119,** 1557–1574.

——, and D. W. Burgess, 1994: Positive cloud-to-ground lightning in tornadic storms and hailstorms. *Mon. Wea. Rev.*, **122,** 1671–1697.

——, ——, V. Mazur, W. D. Rust, W. L. Taylor, and B. C. Johnson, 1989: Lightning rates relative to tornadic storm evolution on 22 May 1981. *J. Atmos. Sci.*, **46,** 221–250.

Maddox, R. A., K. W. Howard, and C. L. Dempsey, 1997: Intense convective storms with little or no lightning over central Arizona: A case of inadvertent weather modification? *J. Appl. Meteor.*, **36,** 302–314.

Maier, L. M., and E. P. Krider, 1986: The charges that are deposited by cloud-to-ground lightning in Florida. *J. Geophys. Res.,* **91,** 13 275–13 289.

Maier, M. W., and E. P. Krider, 1982: A comparative study of the cloud-to-ground lightning characteristics in Florida and Oklahoma thunderstorms. Preprints, *12th Conf. on Severe Local Storms*, San Antonio, TX, Amer. Meteor. Soc., 334–337.

Marshall, T. C., 1993: A review of charges on thunderstorm precipitation particles. *Eos, Trans. Amer. Geophys. Union,* **74,** 153.

——, and W. P. Winn, 1982: Measurements of charged precipitation in a New Mexico thunderstorm: Lower positive charge centers. *J. Geophys. Res.*, **87,** 7141–7157.

——, and W. D. Rust, 1991: Electric field soundings through thunderstorms. *J. Geophys. Res.*, **96,** 22 297–22 306.

——, ——, and M. Stolzenburg, 1995: Electrical structure and updraft speeds in thunderstorms over the southern Great Plains. *J. Geophys. Res.*, **100,** 1001–1015.

Mazur, V., J. C. Gerlach, and W. D. Rust, 1986: Evolution of lightning flash density and reflectivity structure in a multicell thunderstorm. *J. Geophys. Res.*, **91,** 8690–8700.

——, X. M. Shao, and P. R. Krehbiel, 1998: ''Spider'' lightning in intracloud and positive cloud-to-ground flashes. *J. Geophys. Res.*, **103,** 19 811–19 822.

Orville, R. E., 1994: Cloud-to-ground lightning flash characteristics in the contiguous United States: 1989–1991. *J. Geophys. Res.*, **99,** 10 833–10 841.

——, and A. C. Silver, 1997: Lightning ground flash density in the contiguous United States: 1992–95. *Mon. Wea. Rev.*, **125,** 631–638.

Peckham, D. W., M. A. Uman, and C. E. Wilcox Jr., 1984: Lightning phenomenology in the Tampa Bay area. *J. Geophys. Res.*, **89,** 11 789–11 805.

Piepgrass, M. V., E. P. Krider, and C. B. Moore, 1982: Lightning and surface rainfall during Florida thunderstorms. *J. Geophys. Res.*, **87,** 11 193–11 201.

Reap, R. M., and D. R. MacGorman, 1989: Cloud-to-ground lightning: Climatological characteristics and relationships to model fields, radar observations, and severe local storms. *Mon. Wea. Rev.*, **117,** 518–535.

Rhodes, C. T., X. M. Shao, P. R. Krehbiel, R. J. Thomas, and C. O. Hayenga, 1994: Observations of lightning phenomena using radio interferometry. *J. Geophys. Res.*, **99,** 13 059–13 082.

Richard, P., and G. Auffray, 1985: VHF–UHF interferometric measurements: Applications to lightning discharge mapping. *Radio Sci.*, **20,** 171–192.

Rust, W. D., R. Davies-Jones, D. W. Burgess, R. A. Maddox, L. C. Showell, T. C. Marshall, and D. K. Lauritsen, 1990: Testing a mobile version of a Cross-chain Loran Atmospheric Sounding System (M-CLASS). *Bull. Amer. Meteor. Soc.*, **71,** 173–180.

Saunders, C. P. R., and I. M. Brooks, 1992: The effects of high liquid water content on thunderstorm charging. *J. Geophys. Res.*, **97,** 14 671–14 676.

——, W. D. Keith, and R. P. Mitzeva, 1991: The effect of liquid water on thunderstorm charging. *J. Geophys. Res.*, **96,** 11 007–11 017.

Seimon, A., 1993: Anomalous cloud-to-ground lightning in an F5 tornado-producing supercell thunderstorm on 28 August 1990. *Bull. Amer. Meteor. Soc.*, **74,** 189–203.

Stolzenburg, M., 1994: Observations of high ground flash densities of positive lightning in summertime thunderstorms. *Mon. Wea. Rev.*, **122,** 1740–1750.

——, W. D. Rust, B. F. Smull, and T. C. Marshall, 1998a: Electrical structure in thunderstorm convective regions. Part I: Mesoscale convective systems. *J. Geophys. Res.*, **103,** 14 059–14 078.

——, ——, and T. C. Marshall, 1998b: Electrical structure in thunderstorm convective regions. Part II: Isolated storms. *J. Geophys. Res.*, **103,** 14 079–14 096.

——, ——, and ——, 1998c: Electrical structure in thunderstorm convective regions. Part III: Synthesis. *J. Geophys. Res.*, **103,** 14 097–14 108.

Uman, M. A., 1987: *The Lightning Discharge*. Academic Press, 377 pp.

Warwick, J. W., C. O. Hayenga, and J. W. Brosnahan, 1979: Interferometric directions of lightning sources at 34 MHz. *J. Geophys. Res.*, **84,** 2457–2468.

Weber, M. R., R. Boldi, P. Laroche, P. Krehbiel, and X. Shao, 1993: Use of high resolution lightning detection and localization sensors for hazardous aviation weather nowcasting. Preprints, *17th Conf. on Severe Local Storms*, St. Louis, MO, Amer. Meteor. Soc., 739–744.

Williams, E. R., 1989: The tripole structure of thunderstorms. *J. Geophys. Res.*, **94,** 13 151–13 167.

——, M. E. Weber, and C. D. Engholm, 1989a: Electrical characteristics of microburst producing storms in Denver. Preprints, *24th Conf. on Radar Meteorology*, Tallahassee, FL, Amer. Meteor. Soc., 89–92.

——, ——, and R. E. Orville, 1989b: The relationship between lightning type and convective state of thunderclouds. *J. Geophys. Res.*, **94,** 13 213–13 220.

Workman, E. J., and S. E. Reynolds, 1949: Electrical activity as related to thunderstorm cell growth. *Bull. Amer. Meteor. Soc.*, **30,** 142–144.

Ziegler, C. L., and D. R. MacGorman, 1994: Observed lightning morphology relative to modeled space charge and electric field distributions in a tornadic storm. *J. Atmos. Sci.*, **51,** 833–851.